The Role of Polar Regions in Global Climate, and a New Parameterization of Global Heat Transport

RICHARD S. LINDZEN AND BRIAN FARRELL

Center for Earth and Planetary Physics, Harvard University, Cambridge, MA 02138

(Manuscript received 29 February 1980, in final form 22 September 1980)

ABSTRACT

Such role as polar regions may have in determining global climate obviously depends on the transport of heat between polar regions and other latitudes. We review the way such transport affects climate sensitivity and stability within the context of simple energy balance models, noting that climate sensitivity in most such models is too small to readily permit the functioning of the Millankovitch mechanism, for example. We then turn to the development of new heat transport parameterizations wherein radiative equilibrium distributions of temperature with latitude are adjusted on the basis of recently noted properties of Hadley cells and baroclinically unstable eddies. The simplest application of this adjustment tends to underestimate the observed pole-equator temperature difference—the error being confined almost entirely to high latitudes (in effect the parameterization overestimates the heat flux). Including the effects of static stability changing with latitude virtually eliminates the discrepancy. This situation is remarkable since heat transport by both stationary waves and ocean currents has been ignored. The implications of this are discussed. Moreover, it is found that climate sensitivity and stability for the new transport parameterization can be different from what is obtained with simpler models, and appears capable of simulating the sensitivity called for by existing climate data.

1. Introduction

Much that we identify with climate is closely associated with polar behavior; ice ages being the most obvious example. The question nonetheless remains as to how polar regions interact with the rest of the earth. Clearly, in a world governed by local radiative equilibrium there would be no interaction. Transport is necessary in order that the polar thermal state can be communicated with the rest of the planet. Thus, an understanding of the transport of heat between different latitudes is central to understanding the role of polar regions in global climate.

In Section 2 of this paper we will review some results from energy balance climate models in order to identify the general role of transport. In Section 3 we describe a physical approach to modeling transport due to Hadley cells and baroclinic instabilities. These mechanisms alone appear capable of accounting for the total observed heat flux without considering heat fluxes due to either stationary waves or ocean currents. The possible implications of this finding are discussed. It should be noted that our approach provides the first simple (and fairly accurate) prediction of the pole-equator temperature difference from first principles and without disposable parameters. We parameterize heat fluxes in terms of radiative forcing rather than surface temperature. The latter, in fact, is a consequence of the various heat transport mechanisms, and not really what is forcing the eddies. Practical difficulties in relating heat flux to temperature gradients have already been noted by Lorenz (1979). Similar problems do not arise in the present parameterization.

In Section 4 our heat flux parameterization is critically assessed. It is found to have important shortcomings in polar regions where too much heat flux is predicted. It is shown that the inclusion of the latitude variation of the static stability of the lowest 2 km of the atmosphere (omitted in Section 3) largely eliminates these shortcomings. Our work, however, does not, as yet, establish the origin of the variations in static stability. This matter is of substantial importance to the determination of climate stability and sensitivity. When, for example, the latitude variation of static stability is held fixed regardless of the position of the ice line, we obtain results similar to other studies of climate stability. In particular, the polar regions are too insensitive to the global heat budget to allow the operation of the Millankovitch mechanism for ice ages. When, however, the distribution of static stability follows the position of the ice line, then sensitivity is greatly increased. Data for climatic trends over the last century support a high sensitivity.

2. General role of heat transport

Following Lindzen and Farrell (1977), we will study the role of heat transport in the context of

0027-0644/80/122064-16$08.00
© 1981 American Meteorological Society

Unauthenticated | Downloaded 10/24/21 12:58 PM UTC

one-dimensional energy balance models of the sort developed by Budyko (1969) and Sellers (1969). Such models deal with a surface heat balance wherein all terms may be either externally specified or represented as a function of surface temperature. Restricting ourselves to steady equilibria, such models lead to equations of the form

$$Qs(x)\mathcal{A}(x,x_s) - (A + BT) + F[T] = 0, \quad (1)$$

where

T	surface temperature
$F[T]$	divergence of dynamic heat flux, F representing some operator
x	$\sin\phi$
ϕ	latitude
x_s	value of x at ice-snow/ice-free, snow-free boundary
$Qs(x)\mathcal{A}(x,x_s)$	solar input
Q	solar constant ÷ 4
$s(x)$	normalized distribution of incoming radiation
$\mathcal{A}(x,x_s)$	1 − albedo
$A + BT$	linearization of infrared cooling of surface. (2)

A suitable approximation to the annual average form of $s(x)$ is

$$s(x) = 1 - 0.482P_2(x),$$

where

$$P_2(x) = \tfrac{1}{2}(3x^2 - 1). \quad (3)$$

For $\mathcal{A}(x,x_s)$, we usually use

$$\mathcal{A} = \begin{cases} a_0 + a_2P_2(x), & x < x_s \\ b_0, & x > x_s, \end{cases} \quad (4)$$

where the term $a_2P_2(x)$ crudely includes the zenith angle dependence of the albedo (Hartmann and Short, 1979).

Various values have been suggested for the constants in (2) and (4). Two sets of choices which span the most commonly used values are given in Table 1. The first set of values is close to what was used by Budyko (1969), Sellers (1969), Held and Suarez (1974), and North (1975), while the second set was used by Hartmann and Short (1979) and derived from an analysis by Oerlemans and Van den Dool (1978). We shall later consider the dependence of climate models on these parameter choices.

For $F[T]$, Sellers (1969) suggested

$$F[T] = \frac{d}{dx}(1 - x^2)D\frac{dT}{dx}, \quad (5)$$

while Budyko (1969) suggested

$$F[T] = -C(T - \bar{T}), \quad (6)$$

where

$$\bar{T} = \int_0^1 T dx.$$

TABLE 1. Two sets of radiative parameters. See text for details. The first set will be referred to as B-S (Budyko-Sellers), and the second as H-S (Hartmann-Short).

	a_0	a_2	b_0	A (W m^{-2})	B [W m^{-2}(°C)$^{-1}$]
B-S	0.7	0	0.4	211.2	1.55
H-S*	0.697	−0.175	0.38	205	2.23

* Based on Oerlemans and Van den Dool (1978).

D and C are constants which are adjusted so that (1) simulates the currently observed $T(x)$. Eqs. (5) and (6) are *ad hoc* parameterizations which are fundamentally dependent on an adjustable parameter. In Section 3 we will attempt to replace (5) and (6) with explicitly physical parameterizations which ideally will be free of disposable constants.

As shown in Lindzen and Farrell (1977), (1) may be solved to obtain the dependence of x_s on Q. To do this one must identify x_s with a particular T_s. One usually adopts $T_s = -10$°C. Parameterization (6) allows a discontinuity in T at $x = x_s$ which leads to a certain arbitrariness in the determination of x_s—but some fix (such as using the mean T at x_s) is generally obvious. The calculational procedure involves (i) selecting x_s; (ii) solving (1) for $T(x)$; and (iii) adjusting Q until $T(x_s) = -10$°C. By moving x_s from 1 to 0 one obtains the complete dependence of x_s on Q (or vice versa). Q is formally identified with the solar constant; however, it is more appropriate to simply regard it as a measure of the global heat budget. Changes in Q can result from seasonal effects, changes in global cloud cover, etc. The dependence of x_s on Q is a general measure of the sensitivity of polar climate to global heat balance.

We shall now review some results of previous studies concerning the dependence of x_s on Q. Let us first consider the case $F[T] \equiv 0$. We shall refer to the temperature distribution so obtained as the *radiative equilibrium distribution* $T_e(x)$. Fig. 1 (taken from Held and Suarez, 1974) shows the variation in θ_0 ($= \sin^{-1} x_s$) with q (a measure of Q). Because of the discontinuity in T at x_s, we have two curves. For both curves a reduction in q leads to an equatorward advance of x_s. As explained in Lindzen and Farrell (1977), this implies a *stable climate*, and comparisons of Fig. 1 with subsequent results will show that the resulting climate is, indeed, very stable. For reference purposes an advance of θ_0 from 72° ($x_s = 0.95$, present value) to 50° ($x_s = 0.77$) requires a 30% reduction in Q. Fig. 2 (taken from Hartmann and Short, 1979) compares $Q(x_s)$, using (5), for both choices of parameters in Table 1. For both choices D was independently chosen to simulate present conditions. Note first that with $F[T] \neq 0$, $Q(x_s)$ has a minimum at some $x_s = X$. For $x_s < X$, the climate

Unauthenticated | Downloaded 10/24/21 12:58 PM UTC

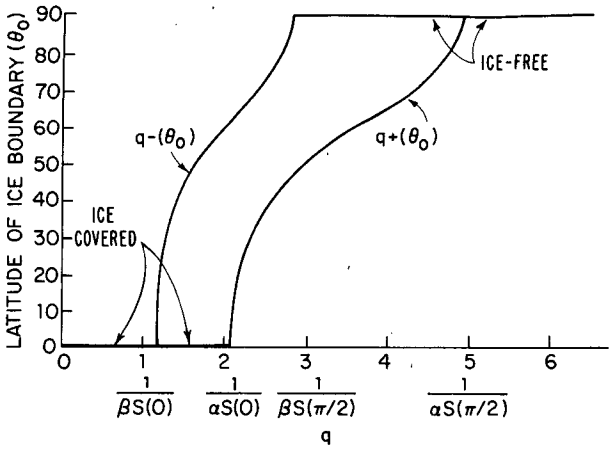

FIG. 1. Variation of a quantity proportional to $Q(q)$ vs θ_0 ($\sin^{-1}x_s$) for radiative equilibrium. The curve q_- represents $T = T_s$ for the ice-free side of x_s while q_+ represents $T = T_s$ for the ice-covered side of x_s. From Held and Suarez (1974).

is *unstable* and perturbations away from equilibrium lead to an ice-covered earth. Note that the choice of parameter set 2 from Table 1 leads to a far less sensitive climate than parameter set 1. For the latter a 2% reduction in Q causes x_s to advance from 0.95 to 0.77 while for the former such an advance requires an 8% reduction. Both cases, however, are far more sensitive than they would be in the absence of transport. In order to explain why results differ for the two parameter choices, let us turn to Fig. 3 (from Lindzen and Farrell, 1977) which shows $Q(x_s)$ based on (5) and parameter set 1, but with different choices for D (no attempt was made to simulate present conditions). We see that the larger D/B is (i.e., the more effective transport is) the more sensitive x_2 is to variations in Q. Indeed for sufficiently large D/B, the climate is everywhere unstable. Finally, Fig. 4 shows $T_e(x)$ (radiative equilibrium) for the two parameter set choices; also shown is the observed $T(x)$. Clearly, $T(x)$ has a much smaller pole-equator temperature difference than either $T_e(x)$. However, for parameter set 1, $T_e(x)$ is substantially colder near the pole than it is for set 2. Thus for set 1 a larger D/B is needed in order to simulate existing conditions, and from Fig. 3 we see that this implies greater sensitivity—as, in fact, was the case in Fig. 2.

Before continuing let us summarize the results of the above discussion:

1) Transport is essential to the instability of simple climate models. The instability arises from the need for ice-free regions to share their heat with ice-covered regions. This process is obviously more general than the simple models with which it was studied.

2) In models where transport is adjusted to simulate existing conditions, the lower the value of $T_e(x)$ over ice, the greater the need for transport will be, and the more sensitive (less stable) will be the response to variations in Q.

As we have already suggested, the quantity dQ/dx_s is the general measure of sensitivity and stability. As clearly illucidated in Held and Suarez (1974), $dQ/dx_s < 0$ implies instability while $dQ/dx_s > 0$ implies stability. Moreover, when dQ/dx_s is positive, the sensitivity of x_s to the global heat balance (as represented by Q) is inversely proportional to dQ/dx_s. In addition, Held and Suarez showed that for time de-

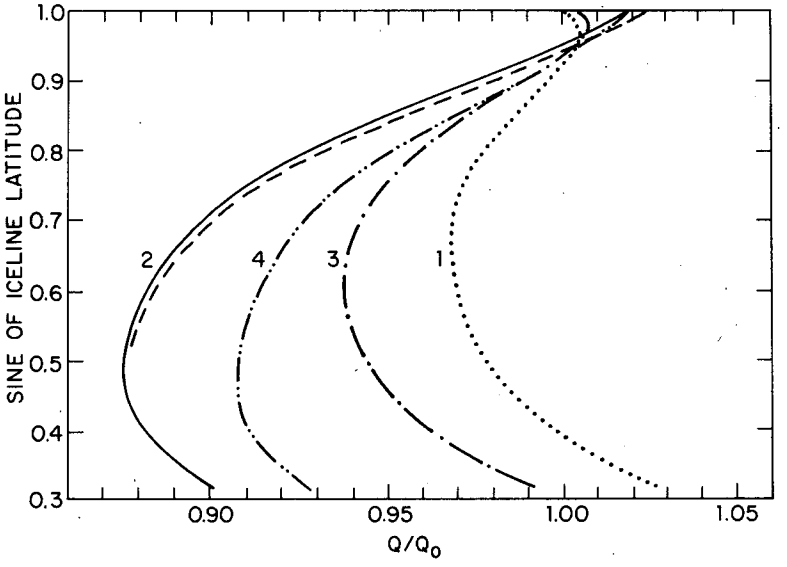

FIG. 2. Q/Q_0 (Q_0 = present value) vs x_s for various choices of radiative parameters. Curve 1 is for the BS parameters; curve 2 is for the HS parameters; curves 3 and 4 are for intermediate choices. From Hartmann and Short (1979).

Unauthenticated | Downloaded 10/24/21 12:58 PM UTC

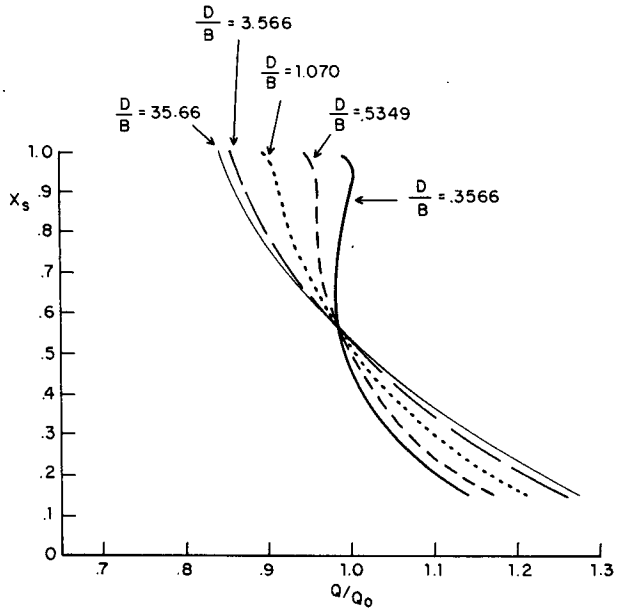

FIG. 3. Q/Q_0 vs x_s for BS radiative parameters and various choices of thermal conductivity. From Lindzen and Farrell (1977).

pendent perturbations away from equilibrium, relaxation rates are proportional to dQ/dx_s. In practical terms, for example, the operation of the Millankovitch mechanism for ice ages (Imbrie, 1979; Suarez and Held, 1976) demands a very small dQ/dx_s—much smaller than obtained with models incorporating flux parameterizations (5) and (6) (Lindzen and Farrell, 1977; North and Coakly, 1979). In a similar vein, various models for climate oscillations have been suggested (Newell, 1974; Saltzman, 1978). A typical schematic for such a model is shown in Fig. 5. Although there is a clear set of negative feedbacks which can lead to a long-period oscillation, the oscillation is damped and the damping, not surprisingly, is proportional to dQ/dx_s. In unpublished calculations by the present author, it was generally found that the high-latitude values of dQ/dx_s in Fig. 2, were so large as to overdamp the oscillations.

In the above, we have identified $(dQ/dx_s)^{-1}$ as a measure of the interaction of polar regions with global climate. This interaction is fundamentally dependent on heat transport, and this motivates our attempt, in the following sections, to develop a physically based parameterization of heat transport.

3. Mechanistic approach to heat transport

In this section we attempt to replace (5) and (6) with parameterizations explicitly based on known physical mechanisms: the tropical Hadley circulation, and baroclinically unstable eddies. Rather than calculate heat fluxes directly we will calculate $\partial T/\partial x$

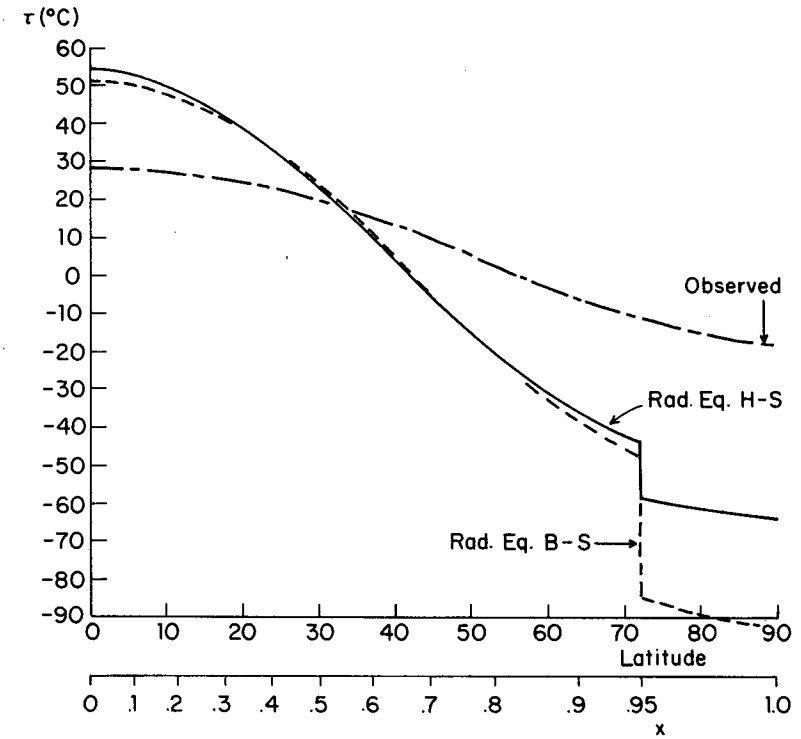

FIG. 4. $T_E(\phi)$ for both HS and BS radiative parameterizations. The observed $T(\phi)$ is also shown. For reference purposes, x as well as ϕ are shown.

Unauthenticated | Downloaded 10/24/21 12:58 PM UTC

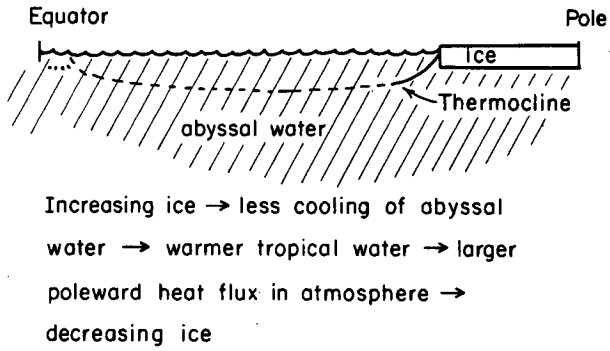

FIG. 5. Schematic illustration of how insulation of deep water by ice could lead to climate oscillation.

as determined by these processes and implement the mechanisms by adjusting $\partial T/\partial x$.

a. Hadley transport

Schneider (1977) has shown that a nonlinear, inviscid, Hadley cell (as schematically illustrated in Fig. 6) is governed by two simple principles:

1) The zonal wind on the poleward branch of the Hadley cell should conserve angular momentum.[1] This implies that u_M, the zonal velocity on poleward branch, is given by

$$\frac{\Omega a \sin^2\phi}{\cos\phi} = \frac{\Omega a x^2}{(1-x^2)^{1/2}}, \tag{7}$$

where Ω is the earth's rotation rate and a the earth's radius.

2) Both u_M and the temperature field must be compatible with the thermal wind relation, which leads to the approximate equation

$$\frac{u_M}{H_{\text{Hadley}}} \approx -\frac{g}{2\Omega \sin\phi \bar{T}}\frac{\partial T}{\partial y} = \frac{g}{2\Omega a \bar{T} x}(1-x^2)^{1/2}\frac{\partial T}{\partial x}, \tag{8}$$

where y is the distance from equator and $\bar{T}$ some characteristic temperature.

Combining (7) and (8) yields

$$\left.\frac{\partial T}{\partial x}\right|_{\text{Hadley}} \approx -\frac{2\Omega^2 a^2 \bar{T}}{g H_{\text{Hadley}}}\frac{x^3}{1-x^2}. \tag{9}$$

A more detailed discussion of these relations may be found in Lindzen (1979) and in Held and Hou (1980). One uses (9) to adjust $T_e(x)$ in the following manner: At the poleward boundary of the Hadley cell $T_{\text{Hadley}} = T_e(x_h)$, where x_h is chosen so that

$$\int_0^{x_h} (T_{\text{Hadley}} - T_e)dx = 0. \tag{10}$$

Because of (10), the Hadley cell only redistributes heat between $x = 0$ and $x = x_h$, without altering the global mean temperature. The temperature distribution consisting in T_{Hadley} for $0 \leq x \leq x_h$ and T_e for $x_h \leq x \leq 1$ will be called $T_{\text{HE}}(x)$. We turn next to the modification of $T_{\text{HE}}(x)$ by baroclinic processes.

b. Baroclinic adjustment

A common approach to parameterizing the effect of an instability on a basic state is to assume that the basic state is neutralized with respect to the instability. The best known example of this is convective adjustment wherein negative lapse rates are adjusted to zero. Pocinki (1955), and, more recently, Stone (1978) have suggested a similar approach to the effects of baroclinic instability. The suggestion stems from the observation that in *two-level* models, there is a critical shear (and by the thermal wind relation, a critical meridional temperature gradient) which is of the order of the observed shear. The difficulty with this approach stems from the fact that in a continuous (as opposed to two-level) atmosphere, there does not appear to be a critical shear. For a zonal flow profile characterized by a shear $d\bar{u}/dz$ in the lower troposphere, Lindzen and Farrell (1980) have shown that the minimum time scale for exponential growth of inviscid baroclinic eddies (corresponding to maximum growth rate) is given by the approximate formula

$$\min \tau_{\text{growth}} \approx \left(0.31\sqrt{\epsilon}\frac{d\bar{u}}{dz}\right)^{-1}, \tag{11}$$

where

$$\epsilon = \frac{4\Omega^2 \sin^2\phi}{N^2},$$

$$N^2 = \frac{g}{\bar{T}}\left(\frac{\partial \bar{T}}{\partial z} + \frac{g}{Cp}\right).$$

Using the approximate thermal wind relation

$$\frac{d\bar{u}}{dz} = -\frac{g}{f\bar{T}}\frac{\partial \bar{T}}{\partial y},$$

where $f = 2\Omega \sin\phi$, and y is the meridional distance from the equator. Taking for $\partial\bar{T}/\partial z$ a characteristic value of -6.5 K km^{-1}, Eq. (11) simplifies to

$$\min \tau_{\text{growth}} \approx 74 \text{ K day}^{-1}\left(-\frac{\partial \bar{T}}{\partial \phi}\right)^{-1}. \tag{12}$$

It is clear from (12) that, in the absence of damping, instabilities will exist for any negative $\partial\bar{T}/\partial\phi$. However, for very small values of $|\partial\bar{T}/\partial\phi|$, τ_{growth} will

[1] The neglect of friction actually inhibits the role of the Hadley cell in transporting heat. Assuming angular momentum is conserved thus tends to minimize the effect of the Hadley cell.

Unauthenticated | Downloaded 10/24/21 12:58 PM UTC

exceed a characteristic damping time. Thus, taking $\tau = 10$ days to be a characteristic damping time, baroclinic adjustment [using Eq. (12)] would lead to

$$-\frac{\partial \bar{T}}{\partial \phi} = 7.4°\text{C},$$

which, in turn, would imply a pole-to-equator temperature difference of

$$\Delta T\Big|_{\text{eqtr}}^{\text{pole}} \approx 7.4° \times \frac{\pi}{2} = 11.6°\text{C}. \tag{13}$$

As we see from Fig. 4, this is much smaller than observed. Such an adjustment would call for larger heat fluxes than are carried by the sum of all transport processes in the atmosphere and ocean.

Clearly, baroclinic instability is not acting to directly eliminate temperature gradients in the manner envisaged above. As already noted in Lindzen *et al.* (1980), one may neutralize a profile with respect to baroclinic instability with far less heat transport by simply smoothing the surface potential vorticity gradient sufficiently. Before explaining this in greater detail, let us put forth the following *plausible conjecture*:

- Baroclinic eddies will carry only as much heat as would be absolutely necessary to neutralize the flow.

Note that this does not require that the final state be neutral; it is only a statement about the heat flux. In order to determine when a flow is neutralized, we turn to a theorem due to Pedlosky (1964), Charney and Stern (1962), and Bretherton (1966):

THEOREM: Baroclinic instability requires that the meridional gradient of potential vorticity change sign.

In a simple baroclinic flow (where $\bar{u}$ is a function only of z, altitude, and static stability is constant) on a β-plane (where β is the meridional derivative of the Coriolis parameter), the meridional gradient of potential vorticity is proportional to

$$q_y = \left(\frac{\beta}{\epsilon} + \frac{1}{H}\frac{d\bar{u}}{dz} - \frac{d^2\bar{u}}{dz^2}\right), \tag{14}$$

where $\beta = df/dy = (2\Omega/a)\cos\phi$ and H is the density scale height (Charney, 1973). We now consider the flow shown in Fig. 7. Here $d\bar{u}/dz$ is everywhere positive while $d^2\bar{u}/dz^2$ is zero or negative. Thus q_y is superficially positive everywhere, and the flow should be stable. However, as noted in Lindzen and Tung (1978), the nature of the lower boundary condition for baroclinic instability is such as to render $d\bar{u}/dz = 0$ at $z = 0$, which, in turn, implies a positive δ-function contribution to $d^2\bar{u}/dz^2$ at the ground. Thus q_y is negative at the ground and the conditions of the above theorem are satisfied. The situation is schematically illustrated in the insert in Fig. 7. Now consider the possibility that the transition between $d\bar{u}/dz = 0$ at $z = 0$ and the characteristic interior shear is effected over a finite layer wherein q_y is a constant. Let

$$\frac{\beta}{\epsilon} + \frac{1}{H}\frac{d\bar{u}}{dz} - \frac{d^2\bar{u}}{dz^2} = \frac{m}{H}\left(r + \frac{d\bar{u}}{d\tilde{z}} - \frac{d^2\bar{u}}{d\tilde{z}^2}\right) = -a^2\left(\frac{m}{H}\right), \tag{15}$$

where

$$r = \frac{\beta H}{\epsilon m}, \quad m = \frac{d\bar{u}}{dz} \text{ above transition region}, \tag{15a}$$

$$\tilde{u} = (\bar{u}(z) - \bar{u}(0))/mH,$$

$$\tilde{z} = z/H,$$

$$\frac{d\bar{u}}{d\tilde{z}} = \begin{cases} 0 & \text{at } \tilde{z} = 0, \\ 1 & \text{at } \tilde{z} = \tilde{d}. \end{cases}$$

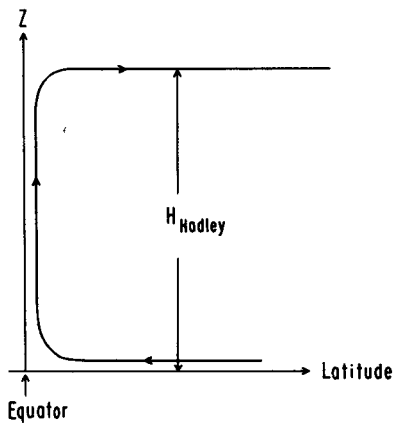

FIG. 6. Schematic illustration of Hadley circulation. The cell ends at an x_h whose determination is described in the text.

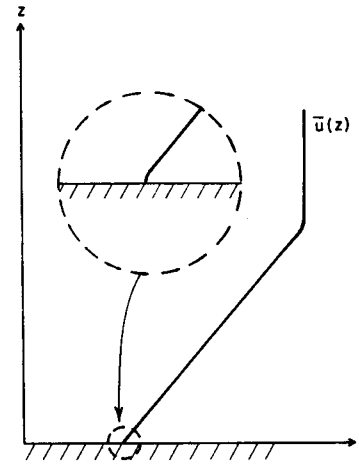

FIG. 7. Typical baroclinically unstable profile of $\bar{u}(z)$. The lower boundary condition interprets $\bar{u}(z)$ in the manner shown schematically in the insert.

Unauthenticated | Downloaded 10/24/21 12:58 PM UTC

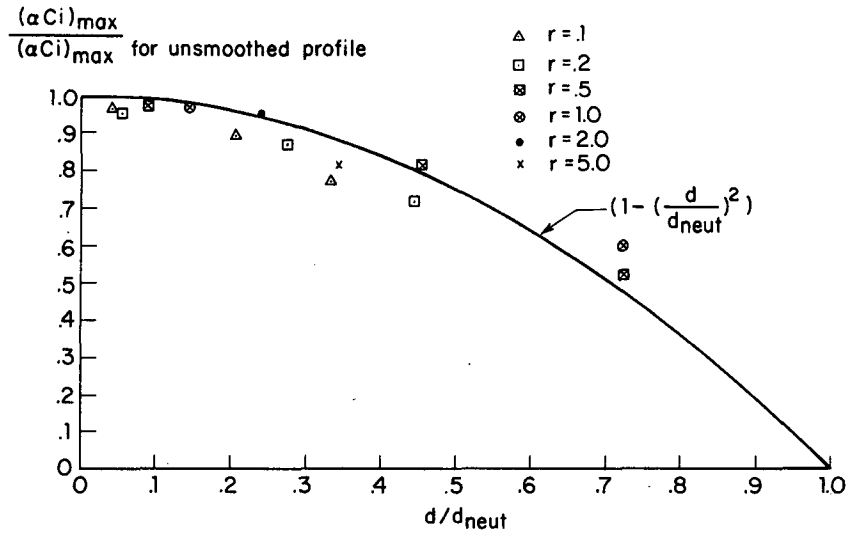

FIG. 8. Normalized maximum growth rate versus d/d_{neut} (the height over which surface potential vorticity gradient is spread). Various symbols represent calculated results at different values of shear for $z > d$ (*viz.*, Fig. 9). Also shown is analytic representation of results.

Since (15) is only 1st order in $d\tilde{u}/d\tilde{z}$, the boundary conditions can only be satisfied at a particular $\tilde{d}$ which will be a function of a^2. Solving (15) one obtains

$$\tilde{u} = -(r + a^2)(\tilde{z} - \tilde{d}) + (1 + r + a^2)e^{(\tilde{z}-\tilde{d})} - (1 + r + a^2), \quad (16)$$

$$\tilde{d} = \ln\left(\frac{a^2 + r + 1}{a^2 + r}\right). \quad (17)$$

When $a^2 = 0$,

$$\tilde{d} = \tilde{d}_{neut} = \ln\left(1 + \frac{1}{r}\right) \quad (18)$$

and the fluid is neutral with respect to baroclinic instability since q_y no longer changes sign in any sense. It already has been noted by Lindzen *et al.* (1980) that the neutralization of the atmosphere by spreading the region of negative q_y until it ceases to be negative involves much less heat flux than implied by neutralization via Eq. (12). Before quantifying this flux, we note that we do not, *a priori*, expect smoothing of the extent given by (18) because, presumably, there exists some smaller $\tilde{d}$ for which maximum growth rates are balanced by dissipation rates. To test this, we calculated the stability properties of an array of profiles with varying $\tilde{d}$ and varying r (nondimensional measure of interior shear).[2] In Fig. 8 we show the variation of the maximum growth rate $(\alpha c_i)_{max}$ divided by $(\alpha c_i)_{max}$ when $\tilde{d} = 0$ [as given by Eq. (12)] versus $\tilde{d}/\tilde{d}_{neut}$ for various choices of r. The profile examined is shown in Fig. 9 and consists a constant tropospheric shear zone, above a transition zone described by (16), blending into a constant $\bar{u}$ stratosphere at $\tilde{z} \equiv \tilde{z}_B = 1.5$. The scatter of points in Fig. 8, in part, may represent inaccuracy in the stability calculations. However, there is no reason to expect *a priori* a universal $(\alpha c_i)_{max}$ vs $\tilde{d}/\tilde{d}_{neut}$ curve independent of r. For example, we may have a dependence on $\tilde{d}/\tilde{z}_B$ (*viz.* Fig. 9). This is especially likely when r is small and $\tilde{d}$ exceeds $\tilde{z}_B$. In such cases, our smoothing procedure is outlined in Fig. 10. These problems could be severe, but for one feature which emerges clearly from Fig. 8: *viz.* $(\alpha c_i)_{max}$ changes slowly until $\tilde{d}/\tilde{d}_{neut}$ is almost equal to 1! That is to say, $\tilde{d}$ must almost

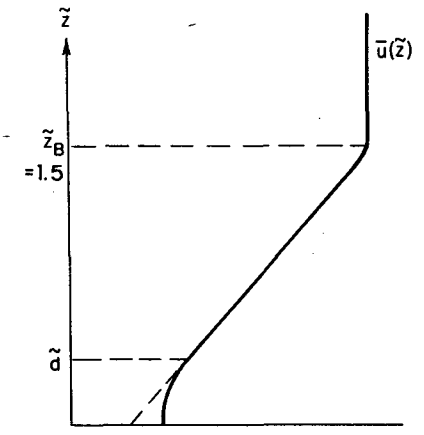

FIG. 9. Schematic illustration of profile examined in connection with Fig. 8

[2] The technique for evaluating stability is essentially given in Lindzen *et al.* (1980).

Unauthenticated | Downloaded 10/24/21 12:58 PM UTC

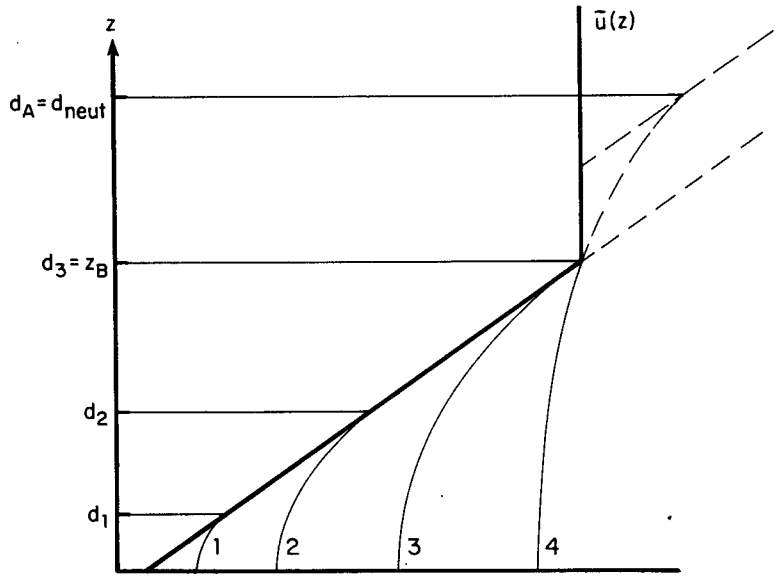

FIG. 10. Schematic illustration of how the region of surface potential vorticity gradient was smoothed when shear was assumed to end above z_B and when d_{neut} exceeded z_B.

equal $\tilde{d}_{neut}$ for neutrality even when we have damping—unless the damping rate is almost comparable to the original growth rate. When the damping rate is as large or larger than the original growth rate, then, of course, we do not expect baroclinic instability to act at all. For our purposes, it suffices to represent the results in Fig. 8 by

$$\frac{\tilde{d}}{\tilde{d}_{neut}} \approx \left(1 - \frac{\tau_{growth}}{\tau_{diss}}\right)^{1/2}, \quad \tau_{diss} \geq \tau_{growth}$$
$$= 0, \quad \tau_{diss} < \tau_{growth}, \quad (19)$$

where τ_{growth} is given by Eq. (12). $\tilde{d}$, as determined from (19) is related to the $\tilde{u}$ profile by (17), (16) and the modification shown in Fig. 10.

As we shall see in the results, the choice of damping time does not appear to be of dominant importance.

With the above results and concepts in hand, we turn, finally, to their implementation in the form of a *baroclinic adjustment* to T_{HE} [*viz.*, Eqs. (9) and (10)].

Given $T_{HE}(x)$, we can calculate dT_{HE}/dx and from the approximate thermal wind relation we can obtain $\partial u_{HE}/\partial z$ as a function of x. This allows the determination of $r(x)$ [Eq. (15a)], $\tilde{d}_{neut}(x)$ [Eq. (18)], τ_{growth} [Eq. (12)] and $\tilde{d}$ [Eq. (19)]. Given $\tilde{d}$, Eq. (16) yields the adjustment to u_{HE} which renders it effectively neutral. Our last step is simply to calculate the mass-weighted average of $\partial u/\partial z$ for this adjusted profile over the height range $0 \leq \tilde{z} \leq \tilde{z}_B$. Simple climate models assume that surface temperature gradients are characteristic of the atmosphere-ocean system as a whole so that radiative heating and cooling as well as atmospheric and oceanic heat fluxes can all be parameterized in terms of the surface temperature (this is discussed in detail in Lindzen and Farrell, 1977). Recall that our present procedure is to determine the *heat flux* implied by baroclinic neutralization. Within the context of simple climate models, the simplest consistent way to introduce this heat flux is to calculate the (mass weighted) average change in $\partial T/\partial y$ (or equivalently, $\partial \tilde{u}/\partial z$) produced by baroclinic neutralization and apply this adjusted $\partial T/\partial y$ to the surface. The heat flux can then be inferred from the radiative imbalance. In practice, the last step is unnecessary since the adjusted temperature gradient is all we need.

For the nondimensional $\partial \tilde{u}/\partial \tilde{z}$, this average will be designated as $\langle \partial \tilde{u}/\partial \tilde{z} \rangle$ and is given by

$$\left\langle \frac{\partial \tilde{u}}{\partial \tilde{z}} \right\rangle = \frac{\int_{-\tilde{d}}^{0} (-(r + a^2) + (1 + r + a^2)e^{\tilde{z}})e^{-\tilde{z}}d\tilde{z} + \int_{0}^{\tilde{z}_B - \tilde{d}} e^{-\tilde{z}}d\tilde{z}}{\int_{-\tilde{d}}^{\tilde{z}_B - \tilde{d}} e^{-\tilde{z}}d\tilde{z}}$$

$$\frac{\dfrac{\tilde{d}}{e^{\tilde{d}} - 1} - e^{-\tilde{z}_B}}{1 - e^{-\tilde{z}_B}} \equiv f(\tilde{d}) \quad \text{for} \quad \tilde{d} \leq \tilde{z}_B, \quad (20a)$$

Unauthenticated | Downloaded 10/24/21 12:58 PM UTC

$$\left\langle \frac{\partial \tilde{u}}{\partial \tilde{z}} \right\rangle = \frac{\int_{-\tilde{d}}^{\tilde{z}_B-\tilde{d}} [-(r+a^2)+(1+r+a^2)e^{\tilde{z}}]e^{-\tilde{z}}d\tilde{z}}{\int_{-\tilde{d}}^{\tilde{z}_B-\tilde{d}} e^{-\tilde{z}}d\tilde{z}} = \frac{1}{e^{\tilde{d}}-1}\left(\frac{\tilde{z}_B}{1-e^{-\tilde{z}_B}}-1\right) \equiv f(\tilde{d}) \quad \text{for} \quad \tilde{d} > \tilde{z}_B. \quad (20b)$$

In terms of dimensional quantities

$$\left\langle \frac{\partial u_{\text{adj}}}{\partial z} \right\rangle = \frac{\partial u_{\text{HE}}}{\partial z} f(\tilde{d}), \quad (21a)$$

$$\left\langle \frac{\partial T_{\text{adj}}}{\partial x} \right\rangle = \frac{\partial T_{\text{HE}}}{\partial x} f(\tilde{d}). \quad (21b)$$

We will refer to $\langle \partial T_{\text{adj}}/\partial x \rangle$ as $\partial T_{\text{BH}}/\partial x$ where T_{BH} is determined by integrating $\partial T_{\text{BH}}/\partial x$ and requiring that

$$\int_0^1 T_{\text{BH}} dx = \int_0^1 T_{\text{HE}} dx = \int_0^1 T_E dx. \quad (22)$$

In Fig. 11[3] we show $\tilde{d}_{\text{neut}}(x)$ and $\tilde{d}(x)$. We will be discussing this figure further in Section 3c. For the moment, we merely note that $\tilde{d}_{\text{neut}}$ and $\tilde{d}$ are close except near the pole. Further, we see that $\tilde{d}_{\text{neut}}$ approximately equals or exceeds $\tilde{z}_b$ for $x > 0.52$ or $\phi > 31°$. These values of $\tilde{d}$ are larger than suggested in Lindzen *et al.* (1980) but recall that the results in Lindzen *et al.* were based on observed vertical shears, while those here are based on the much larger values obtained from the Hadley adjusted radiative equilibria. As can be seen from Eqs. (20a) and (20b), the cessation of shear above z_B leads to greater baroclinic adjustments than would occur if one considered shears continuing to indefinite heights. In Fig. 12 we show T_{BH} for the following cases: Radiative parameters based on each of the parameter sets in Table 1 with $\tau_{\text{diss}} = \infty$, and radiative parameters taken from Hartmann and Short (1979) (i.e., the second set in Table 1) and $\tau_{\text{diss}} = 5$ days. Note that this choice for τ_{diss} represents more dissipation that is regarded as reasonable. We see the following:

(i) T_{BH} is essentially independent of our specific choices of radiative parameters. The differences in Fig. 12 are almost completely attributable to the fact that the two sets of radiative parameters were *not* adjusted so as to yield the same global mean temperature.

(ii) Dissipation does reduce the effectiveness of baroclinic adjustment—but only slightly.

(iii) T_{BH} is quite close to the observed temperature distribution (much closer than T_{HE}), but the predicted pole to equator temperature difference is significantly smaller than observed (32°C vs 46°C); baroclinic adjustment proves more effective than the total observed atmospheric and oceanic heat flux.

Clearly, the discrepancies must be considered further. However, item (iii) above suggests the important possibility (already suggested in Stone, 1978), that baroclinic (and Hadley) transports in the atmosphere can account for the total meridional heat flux. To be sure, other processes contribute to the observed heat flux: ocean heat flux, and heat flux due to forced stationary waves being notable examples. However, these processes, in contrast to baroclinically unstable eddies, do not seem to have the well-defined limiting fluxes described in this paper. It is thus conceivable that these other fluxes simply take up part of the role that baroclinic fluxes would handle if the other transport mechanisms were absent. Baroclinic eddies can then be viewed as a climatic "voltage" regulator, where the pole-to-equator temperature difference plays the role of "voltage". Before turning to both the discrepancies in Fig. 12 and the climatic implications of our results, we turn briefly to the relation of our results to results obtained from two-level models.

[3] As shown in Fig. 11, our Hadley cell ends near $x = 0.6$ ($\phi = 36.8°$). While such an extent is consistent with Schneider (1977), it is greater than usually reported. However, as pointed out by Wallace (1979) most analyses depict the Eulerian meridional circulation which tends to be more confined than the more relevant Lagrangian circulation.

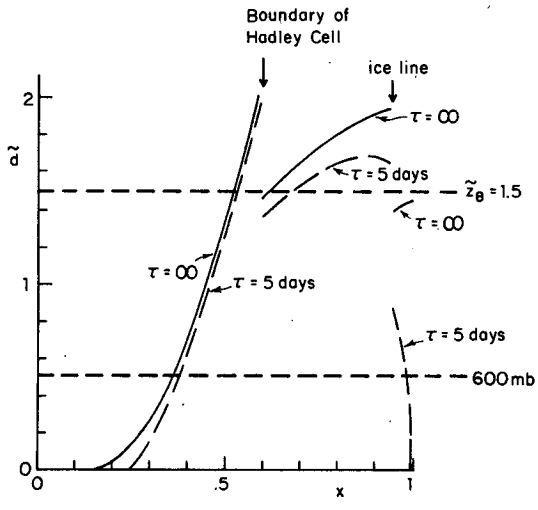

FIG. 11. $\tilde{d}$ vs x without damping [$\tau = \infty$ and $\tilde{d}$ given by Eq. (18)] and with a damping time of 5 days [$\tau = 5$ days and $\tilde{d}$ given by Eq. (19)]. Note that $\tilde{d}$ reaches a maximum at the edge of the Hadley cell (corresponding to the climatological jet stream position), decreasing sharply beyond this point. $\tilde{d}$ also changes sharply at the ice line.

Unauthenticated | Downloaded 10/24/21 12:58 PM UTC

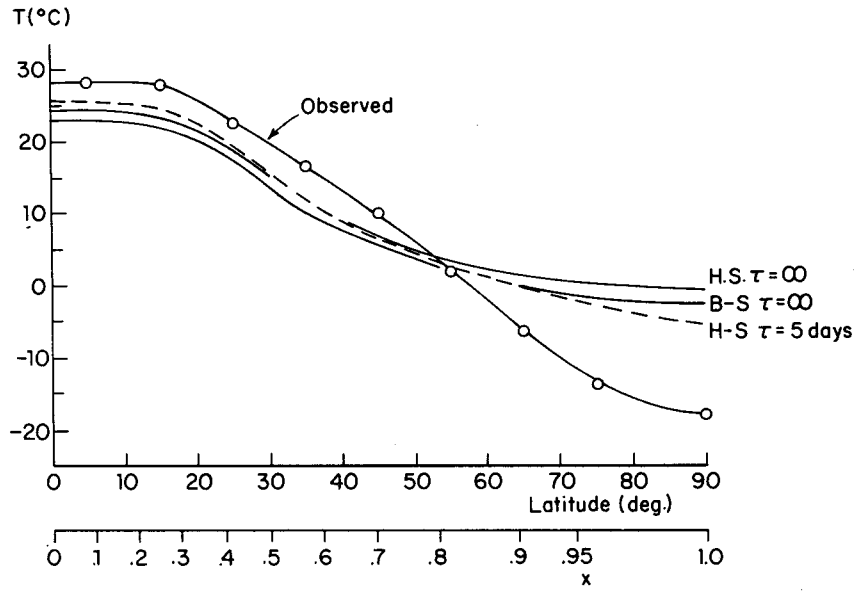

FIG. 12. T_{BH} vs ϕ for HS and BS radiative parameters without dissipation for HS parameters with τ_{diss} = 5 days. Also shown is the observed $T(\phi)$.

c. *Two-level models*

It was noted in the preceding subsection that two-level models possess a critical shear for baroclinic instability—whereas continuous models do not. A close examination of two-level models reveals why. We noted that in a continuous atmosphere baroclinic instability typically depended on the existence of a δ-function contribution to the potential vorticity gradient at the ground and if this contribution were spread over a depth d_{neut}, as given by Eq. (18), the fluid would be neutralized. In a two-level model, the δ-function contribution is *always* spread over the bottom layer. The critical shear in such a model corresponds to that shear at the interface of the two layers for which the smoothing is achieved by a layer with zero potential vorticity gradient. Greater shears lead to a negative potential vorticity gradient in the bottom layer and thus to instability. In Fig. 11 we indicate that value of $\bar{d}$ corresponding to a middle level at 600 mb. It is easily shown from this figure that a baroclinic adjustment consisting in setting $\partial u/\partial z$ to its critical value in a two-level model would lead to a smaller value than that obtained in this paper for the region poleward of ~22°, and to a larger value for the region equatorward of ~22°. These peculiar features of two-level models constitute serious drawbacks to their use in climate modeling.

4. Effect of static stability variations on baroclinic adjustment: Implications for climate

From Fig. 12 we see that our baroclinic adjustment leads to greater heat fluxes than we want, and, in view of the discussion of Section 2, we expect less climatic stability than shown in Fig. 2. This expectation will be quantitatively confirmed later in this section. First, however, we must consider why our baroclinic Hadley adjustment is leading to smaller than observed pole-equator temperature differences. From Fig. 12 we note that our adjustment matches observed temperature gradients ($\partial T/\partial\phi$) almost perfectly (apart from an additive constant) from the equator to 45–50° (from $x = 0$ to about $x = 0.75$, i.e., over ¾ of the earth). The error is almost entirely due to an underestimate of $\partial T/\partial\phi$ poleward of 50°.

While there are certainly questions concerning our basic premises, it is also clear that the procedure proposed in Section 3 was not precisely implemented. Without a more careful implementation, further critical assessment of the basic procedure may not be altogether meaningful. In determining the heat flux needed to neutralize baroclinic instability, we assumed a specified constant value for the static stability. Observationally, this is not the case, at least for the lowest 2 km of the troposphere at high altitudes. The lapse rate diminishes from ~6.5° km^{-1} to zero and even positive values over ice- and snow-covered regions. What we will show, in this section, is that the inclusion of such variable lapse rates in our parameterization significantly alters our results —bringing them into much better agreement with observations. This is consistent with the findings of Held and Suarez (1978). What we will not be able to show is the exact origin of the variable lapse rates. Over ice, it seems likely that local physical processes are of importance. It is also clear, however,

Unauthenticated | Downloaded 10/24/21 12:58 PM UTC

that had we allowed the lapse rate, in addition to $\bar{u}$, to change, it would have been possible to further reduce the heat flux necessary to neutralize the atmosphere with respect to baroclinic instability. (It is clear simply because the use of the observed lapse rate variations reduces the heat flux.) Thus far we have been unable to solve this more complicated extremization problem.

In what follows we will continue to use both the Budyko-Sellers and Hartmann-Short formulations for determining radiative equilibrium surface temperatures. In addition, we will specify the lapse rate as a function of both height and latitudes as follows:

$$\frac{\partial T}{\partial z} = -6.5°\text{C km}^{-1}, \qquad y < y_1, \quad 0 < z < z_b \tag{23a}$$

$$\frac{\partial T}{\partial z} = (-6.5°\text{C km}^{-1})\left(\frac{y_2 - y}{y_2 - y_1}\right), \qquad y_1 < y < y_2; \quad z < z_1 = 0.25H$$

$$= -6.5°\text{C km}^{-1}, \qquad y_1 < y < y_2; \quad z_1 < z < z_b \tag{23b}$$

$$\frac{\partial T}{\partial z} = 0, \qquad y > y_2; \quad z < z_1$$

$$= -6.5°\text{C km}^{-1}, \qquad y > y_2; \quad z_1 < z < z_b. \tag{23c}$$

For y_1 we will take the poleward boundary of our Hadley cell [*viz.*, Eq. (10)]. Recall that this boundary extends well into middle latitudes. We will experiment with the choice of y_2, but the most plausible choice would appear to be the ice boundary. For future reference,

$$y_i = a\phi_i \quad \text{and} \quad x_i = \sin\phi_i.$$

For present purposes we will take (23a)–(23c) to be applicable for both radiative equilibrium and adjusted states. Since static stability (and consequently $\epsilon = f^2/N^2$) now varies with z, Eq. (14) must be replaced by the more general expression

$$q_y = \frac{1}{\epsilon}\left[\beta - \frac{1}{\rho_s}\frac{\partial}{\partial z}\left(\epsilon\rho_s\frac{\partial \bar{u}}{\partial z}\right)\right], \tag{24}$$

where ρ_s the basic density distribution = ρ_s(surface)$e^{-z/H}$. Our calculation of the neutral distribution of $\bar{u}$ and the accompanying adjustment of surface temperature gradient follows lines parallel to those described in Section 3. Details are given in the Appendix. Eq. (11) is now used to calculate growth rates, where ϵ and $d\bar{u}/dz$ are evaluated at the surface. We continue to use (19) for including the role of dissipation.

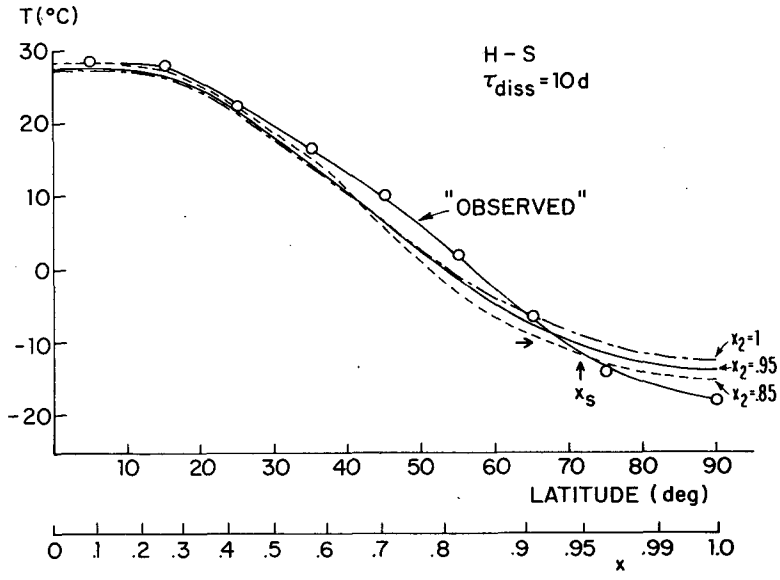

FIG. 13. T_{BH} (corrected for variations in static stability) vs ϕ for HS radiative parameters, τ_{diss} = 10 days, and various choices of x_2 [see Eq. (23)]. Also shown is the observed $T(\phi)$.

Unauthenticated | Downloaded 10/24/21 12:58 PM UTC

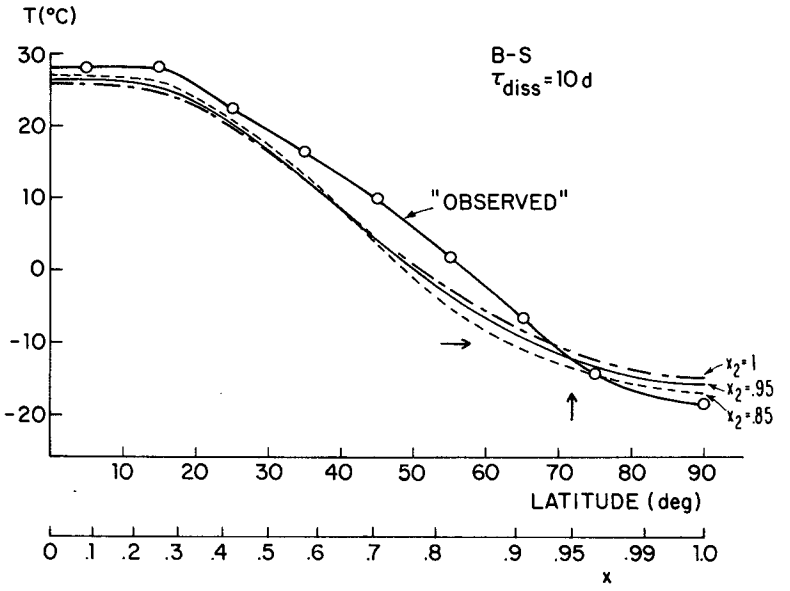

FIG. 14. As in Fig. 13 except BS radiative parameters were used.

Our results for $T_{BH}(\phi)$ are shown in Figs. 13 and 14. We consider $x_2 = 1$ and 0.85 as well as $x_2 = 0.95$ (corresponding to $x_2 = x_s$). In all the calculations shown in Figs. 13 and 14 we have taken $x_s = 0.95$; we have also taken $\tau_{diss} = 10$ days. Comparison with results for $\tau_{diss} = \infty$ are given in Table 2. Fig. 13 shows results using the Hartmann-Short radiative parameterization while Fig. 14 uses the Budyko-Sellers parameterization. In both figures, the observed temperature is shown for comparison purposes. As in Fig. 12, the results for T_{BH} are much the same regardless of the choice of radiative parameterization. The differences can still be attributed to the fact that the two parameterizations do not yield the same global mean temperatures. Indeed, even agreement with the observed temperature could be improved if the radiative models were adjusted to yield the observed global mean temperature. Despite this, the general agreement of the predicted temperatures with the observed temperatures is remarkably good—much better than in Fig. 12. Moreover, as can be seen from Table 2, the agreement does not depend strongly on the choice of τ_{diss}. To be sure, the predicted pole-equator temperature differences are still a few degrees less than observed. This discrepancy is diminished as x_2 is reduced from 1.0 to 0.085. However, the results for $x_2 = x_s = 0.95$ are already entirely acceptable. For example, with $x_2 = x_s = 0.95$, $T_{BH}(x_s)$ is very nearly -10°C ($T_{observed}$, in fact, is significantly less than -10°C). Seeking

TABLE 2. A comparison of $T_{BH}(x)$ with different static stability corrections ($x_2 = 0.85$ and 1.0), both choices of radiative parameters (H-S and B-S), with and without dissipation ($\tau_{diss} = \infty$ and 10 days).

Radiative parameters	x	ϕ (deg)	T_{BH} (°C) with static stability correction			
			$x_2 = 1$		$x_2 = 0.85$	
			$\tau_{diss} = \infty$	$\tau_{diss} = 10$ days	$\tau_{diss} = \infty$	$\tau_{diss} = 10$ days
H-S	0.99	81.9	−10.6	−11.8	−12.7	−14.4
	0.75	48.6	3.77	3.53	2.32	2.1
	0.5	30	17.6	17.6	18.7	18.8
	0.3	17.5	25.1	25.4	26.1	26.5
	0.0	0	26.9	27.3	27.9	28.4
B-S	0.99	81.9	−12.3	−13.6	−14.1	−15.8
	0.75	48.6	1.95	1.73	0.5	0.29
	0.5	30	16.1	16.1	17.2	17.3
	0.3	17.5	23.6	23.9	24.7	25.1
	0.0	0	25.4	25.8	26.5	26.9

Unauthenticated | Downloaded 10/24/21 12:58 PM UTC

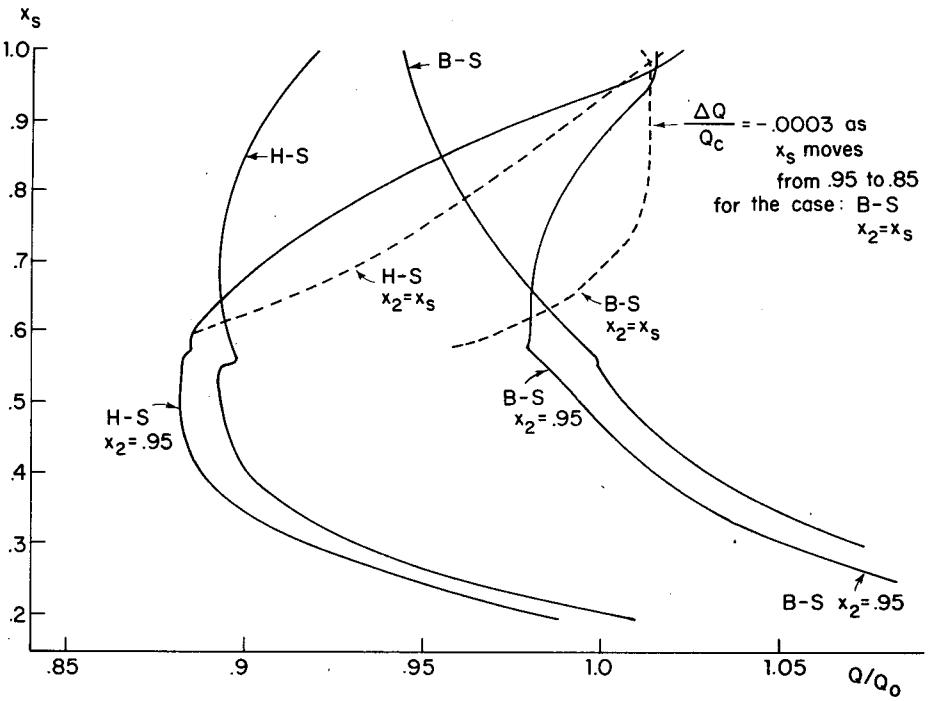

FIG. 15. Q/Q_0 vs x_s for the uncorrected baroclinic-Hadley adjustment, and for the baroclinic-Hadley adjustment corrected for static stability variations with both $x_2 = 0.95$ and $x_2 = x_s$. Calculations with both HS and BS radiative parameterizations are shown. $\tau_{diss} = 10$ days was used.

closer agreement seems unwarranted for at least two reasons:

1) The observed temperature is merely the average between crudely determined winter and summer results (hence the use of quotation marks about observed in Figs. 13 and 14).

2) In a system as nonlinear as the present one, it is unreasonable to expect precise agreement between annually averaged temperatures and the response of the system to annually averaged radiative conditions.

The present results demonstrate the importance of meridional variations in the static stability of the troposphere's lowest 2 km. They are also unique in that agreement with observations was achieved with essentially no disposable parameters. The close agreement strongly supports our suggestion that baroclinic instability acts as a thermal regulator for the zonally averaged climate system.

We turn next to the stability properties associated with baroclinic-Hadley transport as described in Section 3 and modified in the present section. In Fig. 15 we show x_s vs Q/Q_0 for the following three cases (using both Budyko-Sellers and Hartmann-Short radiative parameterizations):

(i) Heat transport described by the unmodified baroclinic-Hadley adjustment of Section 3.

(ii) Baroclinic-Hadley adjustment modified to include effect of variable static stability where $x_2 = 0.95$ regardless of x_s.

(iii) Baroclinic-Hadley adjustment modified as in item (ii), but with $x_2 = x_s$.

For case (iii) no attempt was made to continue calculations to values of x_s less than the poleward edge of our Hadley circulation.

As already suggested, the use of the uncorrected baroclinic-Hadley adjustment (which significantly underestimates pole-equator temperature differences) greatly reduces climate stability; indeed, for Budyko-Sellers parameters we have instability. When account is taken of latitude variations in static stability and x_2 is fixed at a value of 0.95 (realistically simulating the present temperature distribution) we obtain stability results only mildly different from those in Fig. 2 [For example, Fig. 15 shows a small Hadley stabilization (Lindzen and Farrell, 1977) absent in Fig. 2]. At this stage, one would be left with the impression that for a given radiative parameterization, any heat flux parameterization which produces the present $T(\phi)$ will also have the same stability properties. That this is *not* the case is shown by case (iii). Allowing static stability changes (presumably induced by an ice/snow covered surface) to affect baroclinic heat fluxes, leads to a significant reduction of stability (increase of sensitivity) poleward of $x_s = 0.8$ ($\phi_s = 53°$). In fact, for Budyko-Sellers parameters we have weak instability for $x_s > 0.98$ and very

Unauthenticated | Downloaded 10/24/21 12:58 PM UTC

weak stability for $0.85 < x_s < 0.98$. The stability diagram for Budyko-Sellers parameters and case (iii) is strikingly similar to the schematic diagram presented in Lindzen and Farrell (1977) which would readily permit the operation of the Millankovitch mechanism.

5. Concluding remarks

In this paper we have noted the importance of polar regions to global climate depends on global heat transport. Therefore, we have attempted to model and parameterize this transport on the basis of the known physics of both the Hadley circulation and baroclinic instability. This led to a procedure whereby, given a radiative equilibrium distribution of $T_E(\phi)$, one may immediately adjust it to take account of Hadley and baroclinic processes.

This *baroclinic-Hadley adjustment* has several important and noteworthy properties:

1) Heat transports are parameterized in terms of radiative forcing (the true external forcing for the climate system) rather than surface temperature which is an internal consequence of the heat transports.

2) When account is taken of the latitude variation of static stability in the lower troposphere (*viz.*, Section 4), we are able to predict the present pole-to-equator temperature distribution remarkably well with essentially no important disposable parameters. Such agreement is especially interesting since we have taken no account of heat transport due to ocean currents and stationary waves. This suggests that pole to equator temperature differences may be *regulated* by baroclinic instability regardless of the presence of other transport mechanisms.

3) The use of our adjustment together with a plausible relation between static stability and surface ice/snow cover significantly decreases climate stability (or, equivalently, increases climate sensitivity) at high latitudes. With Budyko-Sellers radiative parameters, the sensitivity is sufficiently great to allow operation of the Millankovitch mechanism for ice ages. Sensitivity can also be increased by properly including seasonal variations (Suarez and Held, 1976; North and Coakley, 1979). Such effects can be enhanced by the present process even should less propitious radiative parameters prove appropriate. Observations do support a high sensitivity for high latitudes. Namely, findings by Mitchell (1966) reproduced in Goody (1980) shows that long-term variations in global temperature indeed are greatly magnified at high latitudes.

The present study is obviously preliminary. It does, however, show that heat transport can be effectively parameterized in terms of explicit physical processes, and that such a parameterization can be as simple (in practice) as the *ad hoc* parameterizations currently in use. The present parameterization, moreover, helps account for the high sensitivity of the polar regions to the global heat budget.

Acknowledgments. This research has been supported by the National Science Foundation through Grant ATM-78-23330 and by the National Aeronautics and Space Administration through Grant NGL-22-007-228. Conversations with E. Schneider are acknowledged, as are the helpful referee comments of I. Held. Finally, much of the work in this paper was done by one of the authors (Lindzen) while he was a Lady Davis Visiting Professor at the Hebrew University in Jerusalem, Israel.

APPENDIX

Effect of Static Stability on Baroclinic Adjustment

We let $T_s(y)$ be the surface temperature. For either Hadley adjusted equilibrium or fully adjusted states we assume that Eqs. (23a)–(23c) describe the associated vertical temperature structures—at least for $0 \leq z \leq z_B$. For the former $T_s(y) = T_{s,\mathrm{HE}}(y)$, while for the latter $T_s(y) = T_{s,\mathrm{BH}}(y)$.

Thus

$$T(y,z) = T_s(y) - 6.5^\circ\mathrm{C\ km^{-1}}z, \qquad y < y_1, \tag{A1a}$$

$$T(y,z) = T_s(y) - 6.5^\circ\mathrm{C\ km}\left(\frac{y_2 - y}{y_2 - y_1}\right)z, \qquad z < z_1; \quad y_1 < y < y_2,$$

$$= T_s(y) - 6.5^\circ\mathrm{C\ km^{-1}}\left(\frac{y_2 - y}{y_2 - y_1}\right)z_1 - 6.5^\circ\mathrm{C\ km^{-1}}(z - z_1), \qquad z > z_1; \quad y_1 < y < y_2 \tag{A1b}$$

$$T(y,z) = T_s(y), \qquad z < z_1; \quad y > y_2$$

$$= T_s(y) - 6.5^\circ\mathrm{C\ km^{-1}}(z - z_1), \qquad z > z_1; \quad y > y_2. \tag{A1c}$$

We see from (A1a)–(A1c) that not only does static stability (and hence, ϵ) vary with height, but in the region $y_1 < y < y_2$ so does $\partial T/\partial y$ (and hence $\partial u/\partial z$).[4] These two features require us to modify the details of

[4] To be sure $\partial u/\partial z$ varies with height in the baroclinically neutral state, but as explained in Section 3, the baroclinically neutral state is simply a reference state enabling us to calculate the adjusted value of dT_s/dy.

Unauthenticated | Downloaded 10/24/21 12:58 PM UTC

the adjustment described in Section 3 in a simple, straightforward manner.

The variation of both ϵ, and $\partial u_{\mathrm{HE}}/\partial z$ (for the Hadley adjusted radiative equilibrium) with height requires that (24) be used instead of (14). Consistent with this, (15) is replaced by

$$\beta - \frac{1}{\rho_s}\frac{\partial}{\partial z}\left(\epsilon\rho_s\frac{\partial \bar{u}}{\partial z}\right) = -a^2. \tag{A2}$$

The boundary conditions given by (15a) remain unaltered. Integrating (A2) subject to these boundary conditions yields

$$\frac{\partial \bar{u}}{\partial z} \doteq \frac{(\beta + a^2)H}{\epsilon}\left(\epsilon\rho_s\frac{\partial \bar{u}}{\partial z}\right) = -a^2, \tag{A3}$$

$$\tilde{d} = \ln\left[1 + \frac{\epsilon(\tilde{d},y)}{(\beta + a^2)H}\frac{\partial u_{\mathrm{HE}}}{\partial z}(\tilde{d},y)\right]. \tag{A4}$$

Eq. (A4) differs from (17) (apart from trivial changes of notation) only in that ϵ and $\partial u_{\mathrm{HE}}/\partial z$ are now very simple functions of $\tilde{d}$ itself. In practice, the solution of (A4) is no more difficult than the solution (17). In the absence of dissipation, $\tilde{d}_{\mathrm{neut}}$ is given by (A4) with $a^2 = 0$. With dissipation, Eq. (19) continues to be used to relate $\tilde{d}$ to $\tilde{d}_{\mathrm{neut}}$.

The determination of $\langle \partial\bar{u}/\partial z\rangle$ and its relation to $\partial T_{\mathrm{BH}}/\partial y$ is given by (21a,b) of Section 3 for $y < y_1$ and $y > y_2$. In the region $y_1 < y < y_2$, where the adjusted value of $\partial u/\partial z$ must vary with height (and where $\partial T_{\mathrm{BH}}/\partial y$ varies with height), the relation between $\langle \partial\bar{u}/\partial z\rangle$ and $\partial T_{s,\mathrm{BH}}/\partial y$ is slightly more complicated. From (A1) and the simplified thermal wind relation [given below Eq. (11)] we find

$$\frac{\partial u_{\mathrm{adjusted}}}{\partial z} = \begin{cases} -\dfrac{g}{f\tilde{T}}\left(\dfrac{dT_{s,\mathrm{BH}}}{dy}\right) + 6.5^{\circ}\mathrm{C\ km^{-1}}\left(\dfrac{z}{y_2 - y_1}\right), & z < z_1 \\ -\dfrac{g}{f\tilde{T}}\left(\dfrac{dT_{s,\mathrm{BH}}}{dy}\right) + 6.5^{\circ}\mathrm{C\ km^{-1}}\left(\dfrac{z_1}{y_2 - y_1}\right), & z_1 < z < z_B. \end{cases} \tag{A5}$$

We next take the density weighted average of (A5) with respect to z (for our purposes it is sufficiently accurate to use a constant average value for $g/f\tilde{T}$ to obtain

$$\left\langle\frac{\partial \bar{u}}{\partial z}\right\rangle = -\frac{g}{f\tilde{T}}\frac{dT_{s,\mathrm{BH}}}{dy} - \frac{gH}{f\tilde{T}}\frac{6.5^{\circ}\mathrm{C\ km^{-1}}}{y_2 - y_1}\left(\frac{1 - e^{-\tilde{z}_1} - \tilde{z}_1 e^{-\tilde{z}_B}}{1 - e^{-\tilde{z}_B}}\right). \tag{A6}$$

In the region $y_1 < y < y_2$, (A6) replaces (21a,b) in relating $dT_{s,\mathrm{BH}}/dy$ to $\langle \partial\bar{u}/\partial z\rangle$, $\langle \partial\bar{u}/\partial z\rangle$ having already been calculated from (A3).

REFERENCES

Bretherton, F. P., 1966: Critical layer instability in baroclinic flows. *Quart. J. Roy. Meteor. Soc.*, **92**, 325–334.

Budyko, M. I., 1969: The effect of solar radiation variations on the climate of the earth. *Tellus*, **21**, 611–619.

Charney, J. G., 1973: Planetary fluid dynamics. *Dynamic Meteorology*, P. Morel, Ed. D. Reidel, 97–351.

——, and M. E. Stern, 1962: On the stability of internal baroclinic jets in a rotating atmosphere. *J. Atmos. Sci.*, **19**, 159–172.

Goody, R. M., 1980: Polar process and world climate (a review). *Mon. Wea. Rev.*, **108**, 1935–1942.

Hartmann, D. L., and D. A. Short, 1979: On the role of zonal asymmetries in climate chance. *J. Atmos. Sci.*, **36**, 519–528.

Held, I. M., and M. J. Suarez, 1974: Simple albedo feedback models of the icecaps. *Tellus*, **26**, 613–629.

——, and ——, 1978: A two-level primitive equation atmospheric model designed for climatic sensitivity experiments. *J. Atmos. Sci.*, **35**, 206–229.

——, and A. Hou, 1980: Nonlinear axially symmetric circulations in a nearly inviscid atmosphere. *J. Atmos. Sci.*, **37**, 515–533.

Imbrie, J., and K. P. Imbrie, 1978: *Ice Ages: Solving the Mystery*. Ridely Enslow, 224 pp.

Lindzen, R. S., 1979: On a calculation of the symmetric circulation and its implications for the role of eddies. *The General Circulation*, M. L. Blackmon, Ed., National Center for Atmospheric Research, 257–284.

——, and B. Farrell, 1977: Some realistic modifications of simple climate models. *J. Atmos. Sci.*, **34**, 1487–1501.

——, and K.-K. Tung, 1978: Wave overreflection and shear instability. *J. Atmos. Sci.*, **35**, 1626–1632.

——, and ——, 1980: A simple approximate result for the maximum growth rate of baroclinic instabilities. *J. Atmos. Sci.*, **37**, 1648–1654.

——, ——, and K.-K. Tung, 1980: The concept of wave overreflection and its application to baroclinic instability. *J. Atmos. Sci.*, **37**, 44–63.

Lorenz, E. N., 1979: Forced and free variations of weather and climate. *J. Atmos. Sci.*, **8**, 1367–1376.

Mitchell, J. M., 1966: Stochastic models of air-sea interaction and climatic fluctuation. *Proc. Symp. Arctic Heat Budget and Atmospheric Circulation*, Rand Corp. Memo. RM-5233-NSF, 45–74.

Newell, R. E., 1974: Changes in the poleward energy heat flux by the atmosphere and ocean as a possible cause for ice ages. *Quart. Res.*, **4**, 117, 127.

North, G. R., 1975: Theory of energy-balance climate models. *J. Atmos. Sci.*, **32**, 2033–2043.

——, and J. A. Coakley, Jr., 1979: Differences between seasonal and mean annual energy balance model calculations of climate sensitivity. *J. Atmos. Sci.*, **36**, 1189–1204.

Oerlemans, J., and H. M. van den Dool, 1978: Energy balance climate models: Stability experiments with a refined albedo and updated coefficients for infrared emission. *J. Atmos. Sci.*, **35**, 371–381.

Unauthenticated | Downloaded 10/24/21 12:58 PM UTC

Pedlosky, J., 1964: The stability of currents in the atmosphere and the ocean, Part I. *J. Atmos. Sci.*, **21**, 201–219.

Pocinki, L., 1955: Stability of a simple baroclinic flow with horizontal shear. A. F. Cambridge Research Center, Res. Pap. No. 38, 78 pp.

Saltzman, B., 1978: A survey of statistical-dynamical models of the terrestrial climate. *Advances in Geophysics*, Vol. 20, Academic Press, 183–304.

Schneider, E. K., 1977: Axially symmetric steady-state models of the basic state for instability and climate studies. Part II: Nonlinear calculations. *J. Atmos. Sci.*, **34**, 280–296.

Sellers, W. D., 1969: A global climatic model based on the energy balance of the earth-atmosphere system. *J. Appl. Meteor.*, **8**, 392–400.

Stone, P. H., 1978: Baroclinic adjustment. *J. Atmos. Sci.*, **35**, 561–571.

Suarez, M. J., and I. M. Held, 1976: Modelling climatic response to orbital parameter variables. *Nature*, **263**, 46–47.

Wallace, J. M., 1979: Maintenance of zonally averaged circulation: A. Lagrangian view. *The General Circulation*, M. L. Blackmon, Ed., NCAR, 25–39.

Unauthenticated | Downloaded 10/24/21 12:58 PM UTC